International Journal of Scientific Engineering and Science
Volume 1, Issue 7, pp. 59-64, 2017. ISSN (Online): 2456-7361

An Experimental Analysis of Polarization Shearing Interferometer based Wavefront Sensor

Dr. M. Mohamed Ismail
Assistant Professor, The New College, Chennai, Tamilnadu, India
Email address: mohammedismi@gmail.com

Abstract**—** *A wavefront sensor is the heart of the adaptive optics system. A wavefront sensor in an adaptive optics system, measures the phase changes across the telescope pupil of the incident beam. Adaptive optics works by measuring the distortions in a wavefront sensor and compensating them with a spatial phase modulator such as a deformable mirror. It actively sense and correct the wavefront distortions in the telescope during observations. This paper addresses a real time experiment of Polarized Shearing Interferometer and new developed algorithm for wavefront error estimation. It describes about artificial turbulent medium created in the laboratory and efficient phase extraction algorithm for estimation of the wavefront errors in the Lab VIEW platform.*

Keywords**—** *Babinet Compensator, Polarization Shearing Interferometer, Wavefront Sensor, Adaptive Optics*.

I. INTRODUCTION

In Astronomical Instrumentation, the medium is the Earth's turbulent atmosphere, and the optical signal is the light emitted by the star or the body of interest. The atmospheric turbulence can be considered as a random process and can be estimated by means of variances and co-variances of local refractive index fluctuations [1]. Due to change in the refractive indices of the different layers, the planar wavefront, from the distant star, propagating through the turbulent atmosphere, gets distorted. So, both the amplitude and phase of the incoming beam fluctuate during its passage and changes with time. Thus, the random process of the atmospheric turbulence, affect the image forming capabilities of the telescope. The effects of turbulence on light that passes through the atmosphere are three types.

a. It creates intensity fluctuations or scintillations which are observed as the twinkling of the stars.

b. The position of the star wanders when the varying refractive index of the atmosphere alters the angle of arrival of the starlight.

c. There is a spreading effect created by the higher order aberrations which causes stars to appear as small discs of light and not sharply defined point sources.

The fundamental components of an adaptive optical (AO) system are a wavefront sensor to measure the distortions in the optical beam, a wavefront corrector to compensate these errors, and an estimation and control algorithm to derive the control signals from the distortion measurements.

Shearing Interferometry has the important advantages over other wavefront sensors, it is very high resolution, the interferogram analysis is a global deformation analysis in the Fourier domain and that it requires no reference wavefront for the production of fringes other than the incident wavefront itself i.e. Self-referenced measurement and particularly insensitive to environment vibrations.

In recently some methods based on Lateral shearing interferometry were employed as the wavefront sensor for real time atmospheric corrections [4, 5 and 6]. One of the major drawbacks of these interferometric techniques is the requirement of orthogonal pair of interferograms for wavefront reconstruction but shearing interferometer offers better choice for its linearity, better signal processing and added spatial information. For these advantages a simple lateral shearing interferometer using Babinet compensators (BC) was described in [7]. The technique was further improved employing two crossed BCs [8]. A detailed theory on the use of this PSI device as a wavefront sensor for Adaptive Optics applications was provided [9, 10]. It is important to understand the Polarization Shearing Interferometer (PSI) theoretically to sense the wavefront errors. For this purpose a simulation of wavefront has been generated and incorporated the wavefront errors caused due to atmospheric turbulence with varying noise levels and atmospheric turbulence. The theoretical simulation helps one to understand the behavior of the fringe patterns in different circumstances [11].

In this paper, the work mainly focuses on estimating the wavefront error in real-time based on Polarization Shearing Interferometer - Wavefront Sensor (PSI-WS) technique. The laboratory experimental results which in the presence of turbulence phase plate are presented. An optical design has been worked out for carrying out the experiments with PSI-WS. A turbulence simulator using two rotating phase screens for a realistic condition is used. The actual experiment is performed in an anti vibration isolation table. In order to validate the performance of the wavefront sensor using experimental Polarized Shearing Interferometer based Wavefront Sensor (PSI-WS), laboratory experiments were carried out in the photonics laboratory of Indian Institute of Astrophysics, Bangalore. The details of the optical layout for the measurements and the experimental procedures adopted are presented.

II. TURBULENCE GENERATION

A turbulence simulator using two rotating phase screens is designed to the realization of real observation conditions for adaptive optical instrument. An effort has been put to create a novel means of modelling the spatial and temporal

International Journal of Scientific Engineering and Science
Volume 1, Issue 7, pp. 59-64, 2017. ISSN (Online): 2456-7361

characteristics of phase plates with low cost. Several different technologies using both reflective and refractive methods have been reviewed [12]. The first and natural technique is to use fluid simulators with air or water which is practically complex. Methods such as photo etching [13], near refractive index matching [14], hair spray [15] have been explored with success.

As a first step, we have generated a phase plate by applying oil, and gel between two thin plane parallel glass plates. After the characterisation of those phase plate it is found that these phase plate are not matching well with Kolmogorov model; Secondly, we applied hair spray between the two thin plane glass plates.

A simple optical experiment has been done in order to characterize those phase plates. The implementation of turbulence has been done with hair spray. Hair spray is sprayed on the transparent glass plate in a multiple layers basis with a finite time interval for random turbulence. Two multilayer sprayed glass plates are sandwiched together for better results as shown in the figure 1. For this purpose ordinary hair spray (Gatsby product) has been used. This product contains a component called amphomer, which resembles resin. Dust issues are avoided by sealing the sprayed surface between two plates. For dynamic turbulence behavior, the sandwiched glass plates are rotated with 13 rpm. The hair spray also appears to have good longevity, evident by the turbulence characteristics of sprayed glass plates. The actual experiment is performed on anti-vibration isolation table and the components mounted as per the optical layout as shown in the figure 5.

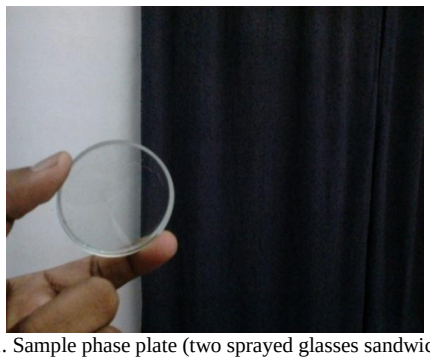

Fig. 1. Sample phase plate (two sprayed glasses sandwiched).

For this experiment, a 30 mm primary telescope aperture has been chosen for the design. In the figure 2 extremely simple turbulent simulator setup is shown. Light coming from the source is collimated by a lens then it is guided to the detector. Now the phase plates are introduced in the collimated beam in order to generate the phase screens as shown in figure 2. Dynamic turbulence is realised by rotating the phase plates with a speed of 13 rpm.

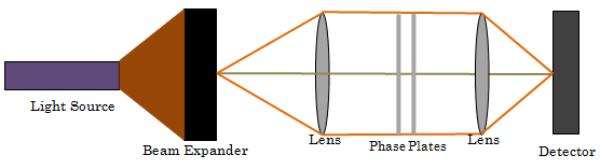

Fig. 2. A Schematic of optical layout for characterising phase screens.

In the figure 3 the experiment has been shown with hair spray, gel and phase plate at the anti vibration table. The collimated beam propagates through the phase plate, and it is distorted. This distorted wavefront is sensed by PixelFly CCD detector for characterisation of phase screens.

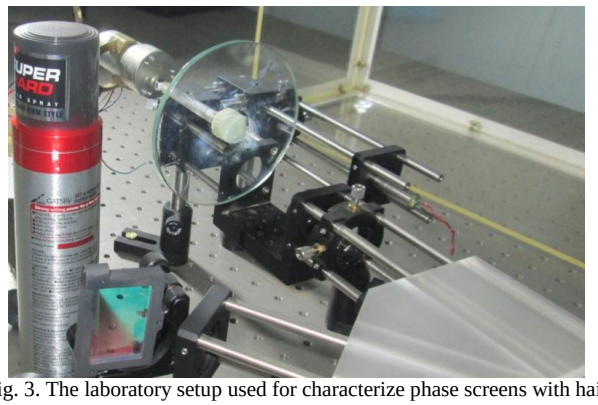

Fig. 3. The laboratory setup used for characterize phase screens with hair spray and phase plate.

Different intensity scale for different configurations improves the contrast. The figure 4.A & B shows the experimental phase screen, which is obtained with turbulent simulator. The figure 4.A shows that the Phase screen obtained when a plane glass plate without hairspray is inserted in the beam path. The figure 4.B shows that the Phase screen obtained when a plane glass plate with hairspray is inserted in the beam path. In this experiment, the phase plates or the phase screens are characterized by measuring the value of the r_0 using the Power Spectrum method. The turbulence model used is based on the Kolmogorov law.

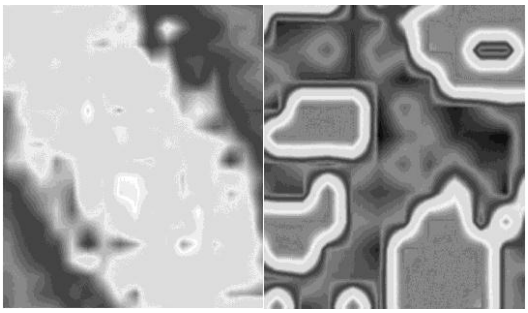

(A) (B)

Fig. 4. Sample phase screen obtained with phase glass plate.

2.1. Power Spectrum Calculation

A way to estimate the Fried parameter is to measure the power spectrum of the phase distortions. The relationship between the phase fluctuations power spectrum W(f) and the Fried parameter r_0 [16] is given by :

$$W(f) = 0.0028\left(r_0^{-5/3} f^{-11/3}\right) \quad 2.1$$

Where f is the spatial frequency. $W(f)$ is related to the OPD δ, by

$$W(f) = \alpha * \langle |FFT(\delta)| \rangle^2 * (\lambda/2\pi)^2 \quad 2.2$$

Where FFT is the Fast Fourier Transform, $\langle |FFT(\delta)| \rangle^2$ is the spectral energy and α is the coefficient converting the spectral energy in power spectrum. $\alpha = N_{tot}\ \tau\ 2$ where N_{tot} is the total number of pixels in the image and τ is the size of the

International Journal of Scientific Engineering and Science
Volume 1, Issue 7, pp. 59-64, 2017. ISSN (Online): 2456-7361

pixels. Using the above equations in LabVIEW, the fried parameter is obtained as a function of f and r_0 value is calculated. It is matching well with the value of r_0 calculated using the Zernike Polynomial method as well as the OTF method.

III. Optical Setup Description

This section describes in detail the laboratory experiment needed to execute the proposed phase extraction algorithm. The laboratory experimental results which were obtained with open loop Adaptive optics system in the presence of turbulence phase plate are presented. If the wavefront error is measured once and corrected once, followed by the acquisition of images, operation is said to be in "open loop". This is also necessary for verifying the efficiency of the algorithm for phase estimation and wavefront reconstruction. It explains about efficient algorithm for estimation of the errors and reconstruction in an open loop system in the Lab VIEW platform.

3.1 Experimental Setup of Polarized Shearing Interferogram

In the laboratory we have undertaken to simulate the turbulence phase screen and to study its effect on the Polarized Shearing Interferometer Wavefront Sensor and to evaluate the Fried's parameter. An efficient approach for shearing interferometry is to separate the two beam by polarization using birefringent prisms. This class of interferometers is called Polarization interferometers. Lateral Shearing Interferometers normally uses two orthogonal shear directions i.e. to measure the slope in two directions in order to reconstruct a two-dimensional wavefront. In laboratory experiment, we have used Babinet Compensator based Polarization Shearing Interferometer which is explained [10]. In [10], he has explained the Polarized Shearing Interferometer using two crossed Babinet Compensator, from that a single interferogram can be efficiently used as a wavefront sensor.

In the laboratory setup a collimated beam is derived from a light source, using a beam expander and a collimating lens. The collimated beam first passes through the test bench where the turbulence phase plates are used for study and next it falls on the Polarization Shearing Device (PSD) Device. A special adapter was fabricated to house the phase plate. The PSD consisting of two crossed Babinet compensators is introduced on either side of the focus (two crossed BC). Neutral Density (ND) filters are used in order to minimize the intensity of the light. The Pixel fly camera has been used to grab the noisy interferometric fringe pattern in the computer. The main parameters in designing the optical system are the position of the Babinet compensator and the detector array size. The schematic of the optical layout for PSI-WS of wavefront sensing experiment at the laboratory is given in the Figure 5. The phase plate was introduced in the optical set up for realistic turbulence and the noisy interferometric image was recorded in to the CCD Detector.

We developed a turbulence simulator at low cost in adaptive optics laboratory. We experimented with several records of the fringe pattern for phase plate evaluation. After characterisation of phase plate it was found that the phase plate is matching well with Kolmogorov model. Also we attempted by both simulation and real time experimentation at lab for comparative analysis.

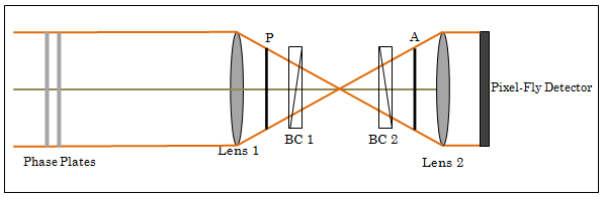

Fig. 5. A Schematic diagram of laboratory setup for Polarization Shearing Interferometer wavefront sensor.

The experimental setup consists of Light Source, Imaging optics, Polarizer, two crossed Babinet Compensator, Analyzer, CCD camera, Control electronics, Control algorithm, Computer and Deformable mirror. The PixelFly Camera has been used as a detector. By using the above set up in the laboratory, the aberrated noisy interferometric image (due to phase plate) is grabbed continuously using PixelFly Camera. The laboratory set up for the measurement using Polarization Shearing Interferometer is shown in Figure 6.

Fig. 6. Photograph of the actual set up.

3.1.1. Light source

A collimated Laser Diode with operating wavelength of 635nm and having 1 mW power light source is used in this experiment. Its beam size is 3 mm. It can withstand large temperature variations. All modules maintain an Optical-to-Mechanical alignment better than 20 mrad.

3.1.2 Imaging optics

It contains Plano-convex lenses with size 30 mm, mirror, with focal length of 50 mm, Pellicle beam splitter of 2 μm size (with reflection 85 and transmission 92 %) and neutral density filters.

3.1.3 Babinet compensator

The Babinet Compensator is widely used as an effective optical device for the measurement of retardation between the ordinary ray (O) and extraordinary ray (e) i.e. to study the degree of birefringence. A Babinet Compensator can be adjusted to provide a variable path difference. The Babinet Compensator consists of paired quartz wedges, of small wedge angle, which are cut in such a fashion that one is positioned with the optic axis parallel to the edge, while the other has the axis perpendicular to the edge. The optical path difference in each wedge increases from the edge to the base and the birefringence has opposite values in the wedges. The

extraordinary axes of the two plates are perpendicular to each other so the roles of the ordinary and extraordinary ray are reversed as the light travels through one plate and then the other. A phase difference or retardation that is accumulated in first wedge may be partially or completely canceled out by second wedge. A dark fringe appears where the net optical phase difference through the compensator becomes zero and a bright fringe when the phase difference is π and continues in a direction at right angles to the zero line as the distance increases. Between crossed polarizer's, dark and bright bands are observed in monochromatic light at a separation distance of one wavelength of optical path difference [10]. A typical Babinet Compensator prisms showing the preferential direction of the optic axis in each prism shown in figure 7.A and BC produced fringe pattern is shown in figure 7.B.

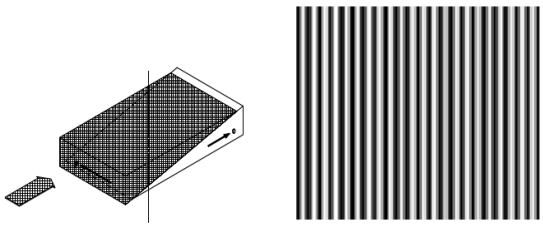

Fig. 7.A. Typical BC, B: Fringe pattern from BC.

3.1.4 Polarized shearing interferometer wavefront sensor device

The polarization shearing device consists of a Polarizer (P), Analyzer (A) and two Babinet compensators (BC) and it is introduced in between the re-imaging optics. The optical specifications of the Babinet compensators are given in the table below.

TABLE 1. Optical specifications of Babinet compensator.

Aperture	15 x 15 mm
Wedge Angle	5 degrees
Material	Quartz
Surface accuracy	$\lambda/20$
Refractive Index Ordinary Ray Extra-ordinary Ray	 1.54424 1.55335

3.1.5 The CCD camera

The CCD camera used here is the PixelFly QE, which is a high performance digital 12bit camera system. The PixelFly has extraordinary quantum efficiency with up to 65%. The system consists of an ultra compact camera head, which either connects to a standard PCI or a compact PCI board via a high speed serial data link. The available exposure times range from 5µs to 65µs. Digital temperature compensation is integrated instead of a space consuming thermo-electrical cooling unit. It has a resolution of 640x480 pixels. The PixelFly camera details are given in table 2.

TABLE 2. PixelFly camera detail.

Details	**Specifications**
Camera Resolution	640X480
Pixel Size	9.9 µm² x 9.9 µm²
imaging frequency, frame rate	177 fps
Dynamic Range	12 bit
pixel scan rate	20 MHz

IV. Experimental Results

The laboratory experimental results which were obtained with open loop Adaptive optics in the presence of turbulence phase plate are presented in this section. Turbulence is simulated by using a sandwiched glass plates they were sprayed by hair spray in a multiple layers. Here the collimated beam passing through turbulent phase plate and due to this distorted wavefront is sensed by PSI Device for wavefront error measurement [17]. This setup is shielded by a glass window in order to minimise the air turbulence. As shown in the figure 8 light passes through a phase plate (which is rotated at 13 rpm for dynamic turbulence behavior) simulated at laboratory, this distorted wavefront is sensed by a PSI-WS and the grabbed image are continuously tested with the proposed algorithm.

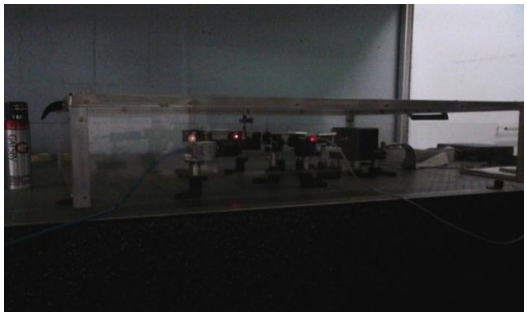

Fig. 8. Adaptive optics setup with turbulent phase plate.

The software for capturing the interferometric images in CCD and analysis of the image is written in the LabVIEW platform. Using this optical setup a typical interferogram has obtained in a PixelFly Camera.

4.1 Data Acquisition Algorithm

The algorithm is developed for image capturing in PixelFly camera for phase aberration estimation. The developed algorithm is used to acquire the image continuously and taken for data reduction procedures. Steps to grab the images from PixelFly camera in LabVIEW are given below.

1. Initialize the PixelFly interface board and camera head. Initialization must be done once for camera in the system.
2. Call Get parameters function which returns camera type, resolution, current gain, binning settings, etc. for the camera.
3. ConFigure the camera for operating mode, trigger mode, exposure time, binning and pixel depth.
4. Call Get Size function which returns maximum and current resolution, along with the pixel depth for the camera configuration.
5. Allocate an image buffer in computer memory. The size of the buffer is specified as the number of bytes required.
6. Map a specified buffer into main memory space, starting at the "buffer address" output. "Buffer address" is then used by the image transfer routines.
7. Start a camera acquisition sequence, placing the camera in wait state until hardware or software trigger is received.
8. Place a buffer in the acquisition queue. If the specified buffer is already in the queue, an error is generated. The queue can hold up to 32 buffers. Once the data has been transferred

International Journal of Scientific Engineering and Science
Volume 1, Issue 7, pp. 59-64, 2017. ISSN (Online): 2456-7361

from the camera to the buffer it is removed from the queue, and the next data transfer will use the next buffer in the queue.
9. Trigger an exposure. If the PixelFly is in internal trigger mode, the exposure starts as soon as this trigger is called. In external trigger mode, the PixelFly waits for a transition on the external trigger input before exposing.
10. Return the status of the selected buffer, including information on queue position.
11. Obtain an image from a buffer and returns it as a 2-D array of 12 bit integers. An array of U16 integers must first be defined that matches the horizontal and vertical dimensions of the image in the buffer. This data format can be used for BW images, using the "Array to IMAQ image" to convert this array to an image.

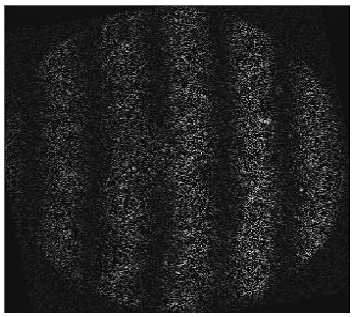
Fig. 9. The interferometric record.

The figure 9 shows that the Interferometric record of the Polarization Shearing Interferometer obtained in the laboratory using PixelFly camera, when turbulence strength is (D/r_o =2). The fringe pattern in the interference is continuously changing due to atmospheric fluctuations (due to phase plate). This changing pattern is a representation of the distortions over the telescope pupil plane. The task is to measure these distortions in real time. The software is developed in such a way that measures the errors in the wavefront and display the wavefront error in real time keeping the cost and time as main factors.

V. Central Fringe Width Localization Algorithm (CFWLA)

After capturing the noisy interferometric image, we extracted the phase using CFWL algorithm. The automated identification in number of fringes technique [18, 19] for the phase extraction from the noisy fringe pattern is reviewed. We proposed and developed with modification in our Central Fringe Width Localization (CFWL) algorithm. It is not possible to find number of fringes and its peak, valley in the noisy interferogram fringe pattern since it have multiple peak and valley in the 1D data.

We approached in different way by adding all column values and averaging of the 2D noisy interferogram data. By doing this we get 1D smooth plot, from this data it is possible to calculate the number of fringes by identify unique peak and valley. The phase differences of the interference field at pixels, where intensity maximum or minimum is located. It is based on the local extrema of the intensity distribution in the interferogram correspond to the extrema of the detected fringes. Automatic techniques for identification of these intensity extrema, i.e. identification of fringe centers, are developed. This approach worked perfectly for calculating the number of fringes with corresponding unique peak and valley identification. After identifying unique peak and valley, we take from valley to valley (single fringe) and fitted into Fourier transform. In the frequency domain we fitted the data into the band pass filter which remove both high and low frequency and allows only frequency band in the middle. The Inverse Fourier transform of the above signal that contains the maximum information was found out to get back the signal in terms of the spatial co-ordinates and the image is filtered for each fringe. The figure 10 shows its noisy 1d data where one cannot locate the peak and valley. The figure 11 shows the compressed and average plot of the noisy data with unique peak and valley identified by CFWL algorithm. The extracted fringe and reconstructed wavefront is shown at figure 12.

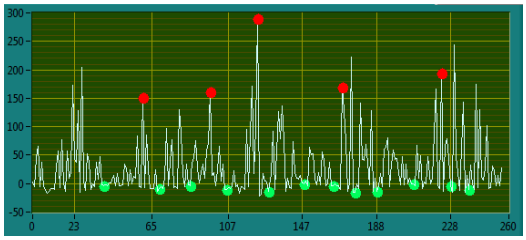

Fig. 10. The 1D noisy interferogram.

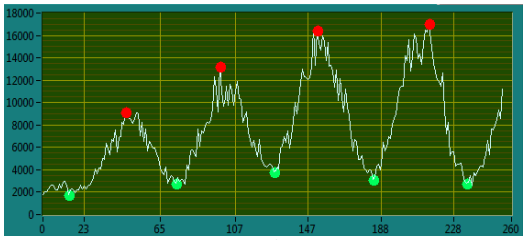

Fig. 11. The compressed 1D noisy interferogram with unique peak and valley identification.

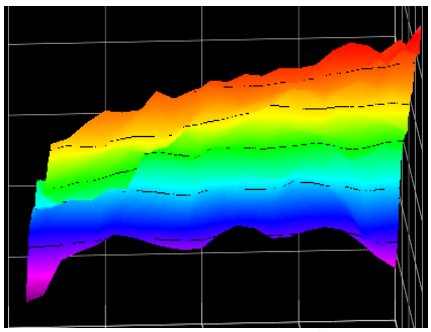
Fig. 12. Reconstructed wavefront.

VI. Conclusion

We have attempted real time experimentation in the laboratory for wavefront error estimation. A low cost turbulent simulator was developed and characterizations of phase screens have been realised in the Laboratory. The CFWLA is tested in the real-time experimental setup with low cost turbulence simulator. Also we have achieved the estimation of wavefront error and reconstruction with reduced time limit.

REFERENCE

[1] J. W. Hardy, *Adaptive Optics for Astronomical Telescopes*, 1998.
[2] J. W. Hardy, J. E. Lefebvre, and C. L. Koliopoulos, "Real-time atmospheric compensation," *Journal of the Optical Society of America*, vol. 67, issue 3, pp. 360-369, 1977.
[3] J. C. Wyant, "Use of an ac heterodyne lateral shear interferometer with real-time wavefront correction systems," *Applied Optics*, vol. 14, no. 11, pp. 2622–2626, 1975.
[4] A. K. Saxena, "Quantitative Test for concave aspheric surfaces using a Babinet Compensator," *Applied Optics*, vol. 18, no. 16, pp. 2897–2901, 1979.
[5] P. Hariharan and D. Sen, "Accurate measurements of phase differences with the Babinet compensator," *Journal of Scientific Instruments*, vol. 37, issue 8, pp. 278–281, 1960.
[6] T. P. Pandya and A. K. Saxena, "An analysis of Babinet Compensator fringes using Jones Calculus," *Kodai. Obs. Bull. Ser. A*, vol. 2, pp. 107–114, 1978.
[7] A. K. Saxena and A. P. Jayarajan, "Testing concave aspheric surfaces: Use of two crossed Babinet Compensators," *Applied Optics*, vol. 20, no. 5, pp. 724-725, 1980.
[8] A. K. Saxena and J. P. Lancelot, "Theoretical fringe profiles with crossed Babinet compensators in testing concave aspheric surfaces," *Applied Optics*, vol. 21, no. 22, pp. 4030–4032, 1982.
[9] A. K. Saxena and J. P. Lancelot, "Wavefront sensing and evaluation using two crossed Babinet compensators," *SPIE*, vol. 1121, Interferometry '89, pp. 41–43, 1990.
[10] J. P. Lancelot, "Wavefront sensing for adaptive optics," PhD Thesis, Indian Institute of Astrophysics, Bangalore, 2007.
[11] M. Mohamed Ismail and M. Mohamed Sathik, "Imaging through Kolmogorov model of atmospheric turbulence for shearing interferometer wavefront sensor," *International Research Journal of Engineering and Technology (IRJET)*, vol. 2, issue 8, pp. 1217-1225, 2015.
[12] D. J. Butler, E. Marchetti, J. Bahr, W. Xu, and S. Hippler, "Phase screens for astronomical multi-conjugate adaptice optics : Applixcation to MAPS," *Proc SPIE*, vol. 4839, pp. 623-634, 2003.
[13] R. Navarro and E. Moreno-Barriuso, "Phase plates for wave-aberration compensation in the human eye," *Optics Letters*, vol. 25, issue 4, pp. 236-238, 2000.
[14] T. A. Rhoadarmer and J. R. P. Angel, "Low-cost broadband static phase for generating atmosphericlike turbulence," *Applied Optics*, vol. 40, issue 18, pp. 2946-2955, 2001.
[15] S. Thomas, *Adavancements in Adaptive Optics*, edited by Domencio Bonaccini calia, Brent l.Ellerbroek of Spie vol 5490.
[16] D. L. Fried, "Optical resolution through a randomly inhomogeneous medium for very long and very short exposures," *Journal of the Optical Society of America*, vol. 56, no. 10, pp. 1372-1379, 1966.
[17] M. Mohamed Ismail and M. Mohamed Sathik, "Fast wavefront reconstruction for interferometric data using LabVIEW," *International Journal of Innovative Research in Computer and Communication Engineering (IJIRCCE)*, vol. 3, issue 11, pp. 10685-10693, 2015.
[18] J. Novák, "Automatic method for detection of interference fringes," Proceedings – Research Activities of Physical Departments of Civil Engineering Faculties in the Czech and Slovak, Republics, Brno 2001.
[19] J. Novák "Interpolation and analysis of interference fringe pattern," Proceedings – Research Activities of Physical Departments of Civil Engineering Faculties in the Czech and Slovak Republics, Brno 2001.